Catalysis Today 289 (2017) 2–13

Contents lists available at ScienceDirect

Catalysis Today

journal homepage: www.elsevier.com/locate/cattod

Synthesis and properties of MCM-41 with polymerizable CADMA cationic surfactant

Laura L. Silva [a], Isabella P. Alkimim [a], Pablo A.S. Vasquez [b], Dilson Cardoso [a,*]

[a] Federal University of São Carlos, Chemical Engineering Department, Catalysis Laboratory, 13565 905, São Carlos, SP, Brazil
[b] Nuclear and Energy Research Institute, Radiation Technology Center, 05508-000, São Paulo, SP, Brazil

ARTICLE INFO

Article history:
Received 21 March 2016
Received in revised form 1 June 2016
Accepted 17 June 2016
Available online 30 June 2016

Keywords:
Cetylallyldimethylammonium bromide
CADMA-MCM-41
Base catalysis
Transesterification
Polymerization by ionizing gamma radiation

ABSTRACT

The synthesis route of MCM-41 was modified by using a cationic surfactant different from the usual CTMABr (cetyltrimethylammonium bromide). This surfactant, cetylallyldimethylammonium bromide (CADMABr), differs from CTMABr by the substitution of a methyl group located in the hydrophilic head by a polymerizable allyl group. The CADMABr surfactant and the CADMA-MCM-41 hybrid silica were synthesized using different times. Formation of the surfactant was confirmed using elemental analysis (CHN), ^{13}C nuclear magnetic resonance (^{13}C NMR), and small-angle X-ray scattering (SAXS) applied to the dispersions of different concentrations of the surfactants in water. The aqueous dispersions of CADMABr and the hybrid silicas were irradiated at different doses of gamma (γ) radiation in order to obtain information about the polymerization of the surfactant. The hybrid silicas were characterized using X-ray diffraction (XRD) for phase identification, together with thermogravimetry (TGA), nitrogen physisorption, and scanning electron microscopy (SEM). The catalytic properties of the silicas were evaluated using the transesterification reaction of monoalcohols as a model for application in biodiesel manufacture.

1. Introduction

For various reasons, currently one of the most studied research themes is the search for alternative sources of energy. In this respect, renewable sources are especially important, including biofuels such as ethanol and biodiesel derived from biomass.

Biodiesel is normally obtained by means of transesterification reactions of vegetable oils or animal fats, which are converted to esters by reaction with a short chain alcohol, producing glycerol as a byproduct. The transesterification reaction most widely used to produce biodiesel involves catalysis by basic sites in a homogeneous medium [1], although it can also proceed in the presence of acidic and enzymatic catalysts. Although the homogeneous phase reaction is fast and provides high conversion rates, it has several negative points, hence motivating a search for alternatives. These points include the difficulty of separating the catalyst after the reaction, which makes the process expensive because it requires neutralization and washing steps to remove residues from the biodiesel. Another disadvantage is that it is not possible to reuse the catalyst in subsequent reactions [2]. For these reasons, a promising alternative is the use of heterogeneous catalysts, which do not suffer from the above-mentioned problems and enable the production of glycerol without contaminating the catalyst [3].

To this end, the use of alkaline earth metal oxides as basic catalysts has been investigated. However, a disadvantage of these materials is their rapid deactivation due to the formation of carbonates in the presence of atmospheric CO_2. One way to avoid carbonate accumulation is to use molecular sieves as basic catalysts [4], since these materials are not affected by the presence of CO_2. They include mesoporous silicas, which offer high activity and have been extensively studied by our research group [4–7].

The synthesis of mesoporous materials of the M41S family was first performed in 1992 by Mobil Oil Corporation scientists [8]. This family consists of three silica structures: MCM-41, MCM-48, and MCM-50 [9]. Of these, MCM-41 (Mobil Composition of Matter number 41) has been most studied. This material has a hexagonal mesoporous structure, with a unidimensional system of pores and a characteristic diffractogram with peaks corresponding to the (100), (110), (200), and (210) planes.

Most of the reported techniques for the preparation of silicas of the M41S family employ a calcination step at the end of the synthesis, in order to eliminate organic cations and empty the mesopores. However, it should be emphasized that the silicas used as basic catalysts are not submitted to this calcination step, because the cations occluded in the pores and present on the external surface of the material are essential for formation of the active catalytic sites.

* Corresponding author.
E-mail address: dilson@ufscar.br (D. Cardoso).

http://dx.doi.org/10.1016/j.cattod.2016.06.041
0920-5861/

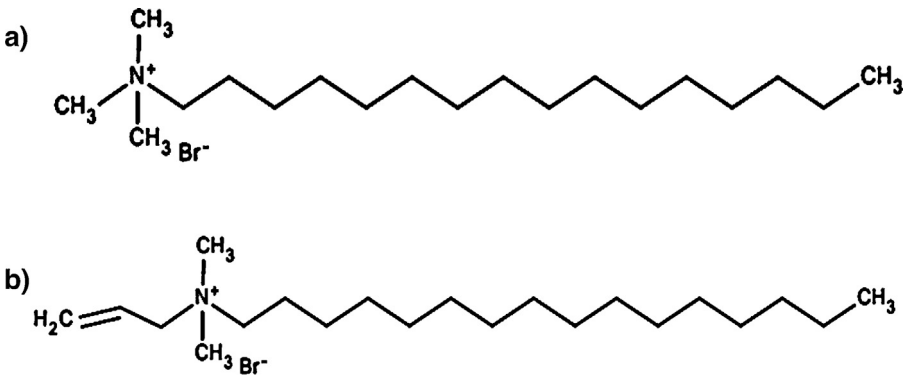

Fig. 1. Surfactants utilized in the synthesis: (a) CTMABr; (b) CADMABr.

This type of material is known as CTMA-MCM-41, due to the presence of the cetyltrimethylammonium (CTMA) cation in the pores of the silica. Materials not submitted to calcination are described as "as-synthesized", and show basic characteristics due to the presence of siloxy (≡SiO^-) anions in the mouths of the pores and on the surface of the material. This concept originated in the article by Kubota et al. [10], and later in the work of Martins et al. [4], who studied the use of this material in the Knoevenagel condensation reaction, and found that it remained active even at temperatures below that of the environment (10 °C). The use of CTMA-MCM-41 in the transesterification reaction has also shown promising results for the transesterification of monoesters as well as vegetable oils [5]. However, when this catalyst is reused, it progressively loses its activity. Martins et al. [4], as well as Fabiano et al. [5], suggested that this loss was caused by the leaching of $CTMA^+$ from the mouth and interior of the pores of CTMA-MCM-41.

More recently, Araújo et al. [6] made modifications to the synthesis of CTMA-MCM-41 with the aim of improving catalytic stability during the course of successive reuses in the transesterification reaction of monoesters. These modifications involved the addition of monomers of the styrene, methacrylate, or acrylate type in the synthesis, together with a photochemical initiator and a polymerization step using ultraviolet light (UVC). The findings were confirmed more recently [7], and the increase in catalytic stability was explained by the formation of polymers in the interior of the micelles contained in the pores of the silica, which inhibited leaching of the CTMA cations.

Given the importance of developing heterogeneous catalysts for the manufacture of biodiesel, and the availability of the modified techniques [6,7], the present work concerns new studies undertaken to improve the properties of these catalysts, without the addition of the monomers described above. It is proposed to substitute the cetyltrimethylammonium bromide (CTMABr) surfactant, used in the synthesis of these mesoporous silicas, by a polymerizable surfactant, cetylallyldimethylammonium bromide (CADMABr), which has not previously been used in the synthesis of MCM-41.

Due to the presence of the cetyl group, in an aqueous dispersion this compound (CADMABr), like CTMABr, assumes the arrangement that is most favorable given its amphiphilic characteristics, grouping in such a way that the apolar tails are directed towards the center away from water, with the polar heads towards the surface. CADMABr differs from CTMABr (Fig. 1a) by substitution of a methyl group for a polymerizable allyl group, as shown in Fig. 1b. Above the critical micellar concentration (CMC) in water, these surfactants form micelles, which is an essential characteristic for mesopores formation in MCM-41.

According to Hamid and Sherrington [11], the polymerization of this type of surfactant forms linear polycations. Thus, if the cation CADMA also gives rise to MCM-41 silica is expected that its polymerization within the pores produces mainly a circular configuration (Fig. 2). This proposal would be another way to increase the stability of cations within the pores of the resultant hybrid silica.

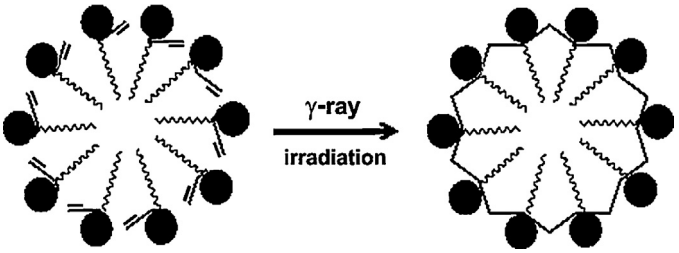

Fig. 2. Representation of CADMA cation polymerization within the pores.

2. Materials and methods

2.1. Synthesis of CADMABr

Cetylallyldimethylammonium bromide (CADMABr) was synthesized by an optimized quaternization reaction [12], with the initial conditions based on previous work [13–15]. The reaction was performed in a round-bottomed flask fitted with a condenser, containing 250 mL of ethyl acetate (Synth, 99%) as the solvent, to which was added equimolar 0.1 mol amounts of *N*,*N*-dimethylhexadecylamine (TCI, 99%) and allyl bromide (Sigma-Aldrich, 99%). The system was kept under stirring at 65 °C for 1 h, followed by 1 h in an ice bath. The CADMABr product was then filtered, washed with ethyl ether (Sigma-Aldrich, 99.5%), and left in a vacuum desiccator for 24 h.

2.2. Synthesis of the hybrid silicas

The hybrid silicas were synthesized using the Schumacher method [16], but without the additional ethanol, as described by Araújo et al. [6] and Cruz and Cardoso [7]. In addition, the usual CTMABr surfactant was replaced by CADMABr. The molar composition of the reaction mixture was: $1SiO_2$:$12.5NH_3$:0.4Surf:$174H_2O$:4EtOH, where Surf represents the CTMABr or CADMABr.

The effect of different synthesis times on the final properties of the silica was evaluated. The nomenclature used for the samples synthesized with CTMABr was as follows: CTXX-Y, where XX is the synthesis time (from 2 to 48 h), and Y refers to the number of uses of the silica in the transesterification reaction (0 or 4 uses). An analogous nomenclature was used for the samples synthesized with CADMABr, substituting the prefix CT for CD.

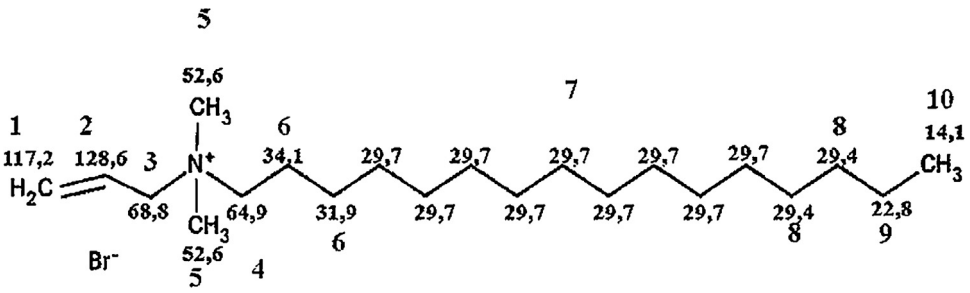

Fig. 3. Chemical shifts of the carbon atoms of CADMABr.

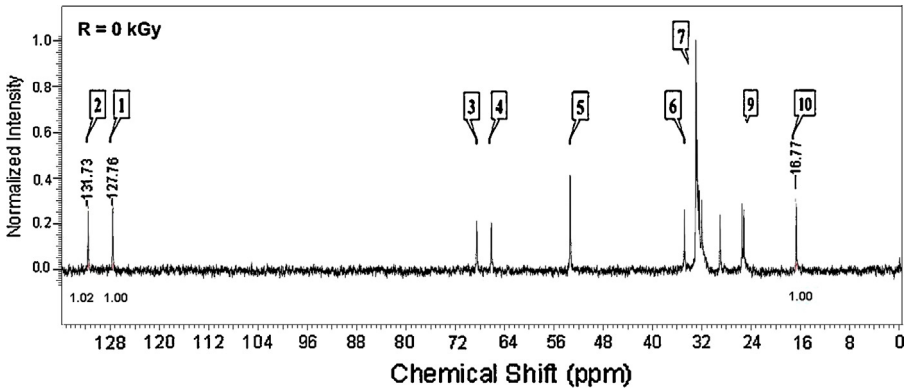

Fig. 4. ^{13}C NMR spectra of the dispersions containing CADMABr non-irradiated (R_0-CADMA).

2.3. Polymerization

Tests of polymerization of the aqueous dispersion of CADMABr [13] and the silicas containing $CADMA^+$ occluded in the pores were performed at the Multipurpose Gamma Irradiation Facility at the Nuclear and Energy Research Institute (IPEN/USP, São Paulo, Brazil). The total installed activity in the facility of Cobalt-60 at the moment of the radiation processing was around 11.1 PBq (300 kCi). The dispersions were prepared with 0.2 mol% CADMABr and stored under an inert atmosphere in sealed 60 ml glass vials. The hybrid silicas were stored in the same way, after drying at 60 °C for 24 h. Then, the solid and liquid samples were irradiated at different doses of gamma radiation. Usually absorbed dose is represented in kilogray (kGy).

The nomenclature used for the liquid samples with CADMABr subjected to gamma radiation is as follows: R_d-CADMA, where R_d indicates the irradiated samples exposed to gamma radiation at different doses (d) (0, 16, 48, 88, 128, and 160 kGy). In the case of the irradiated silicas, R_d is added to the nomenclature described in the previous section (CTXX-R_d-Y, where d corresponds at the doses of 48 or 128 kGy).

2.4. Characterization of the materials

The synthesis of CADMABr was confirmed using elemental chemical analysis of carbon, hydrogen, and nitrogen (CHN), as well as ^{13}C nuclear magnetic resonance (^{13}C NMR). The CHN analyses were performed using a CHNS/O Analyzer 2400 Series II (Perkin Elmer) and the NMR measurements employed a Bruker AVANCE III instrument (9.4 T, 400 MHz hydrogen frequency) equipped with a 4 mm CP/MAS probe for solid samples.

The degree of polymerization of the aqueous dispersions of CADMABr was estimated using ^{13}C nuclear magnetic resonance (^{13}C NMR). This employed the ratio of the areas of the chemical shift peaks at 127 and 131 ppm, corresponding to C1 and C2 of the C=C double bond, respectively, and the peak at 17 ppm, corresponding to the carbon of the methyl group of the hydrophobic tail (C10 in Fig. 3), according to Eq. (1).

$$y = \frac{(2 \times A_{2i}) - A_{1i}}{2 \times A_{2i}} \times 100 \quad (1)$$

where: i = dose of gamma radiation to which the sample was subjected; $A1_i$: sum of the areas of the olefinic carbons (C=C), with $A1_0 = 2$; $A2_i$: area of the methyl carbon of the tail (CH_3), with $A2_i = 1$; Y: degree of polymerization (%).

The area integrations were performed using the free software *ACD/NMR Processor Academic Edition*.

Colloidal dispersions of CTMABr and CADMABr in water were characterized by small-angle X-ray scattering (SAXS), at the SAXS2 beamline at the Brazilian National Synchrotron Light Laboratory (LNLS). This analysis used a wavelength (λ) of 0.1549 nm, a sample-detector distance of 562.5359 mm, and an acquisition time of 300 s (2 × 150 s). The equation describing the scattering (q) and the Bragg equation were used to obtain the equation for calculation of the intermicellar distance (Eq. (2)) [17] for the liquid samples of the two surfactants, where 2θ is the scattering angle relative to the direction of the incident radiation, and λ is the wavelength of the radiation used:

$$d_{\text{int}\,ermicellar} = \frac{2.\pi}{q_{\max}} \quad (2)$$

The hybrid silicas were characterized by X-ray diffraction (XRD) in order to identify the phase formed. A Rigaku Multiflex diffractometer was used, with Cu Kα radiation (40 kV, 40 mA), goniometer speed of 0.5° min^{-1}, and scanning range of $1 < 2\theta < 10°$. For quantification of the degree of organization of the hybrid silicas, the same sample holder was used in all the XRD analyses. Eq. (3) was used to calculate the interplanar distance of the (100) plane, relative to the characteristic plane of the silicas (in nm).

$$d_{100} = \frac{0.15418}{2 \cdot \sin(\theta)} \quad (3)$$

Table 1
Results of CHN analysis of the synthesized surfactant (%, m/m).

Sample	N(%)	C(%)	H(%)
Theoretical	3.3	61.0	10.6
Experimental	3.1	61.2	11.3

Using this technique, it was also possible to determine the degree of organization (DO%) of the silicas, relative to the (100) plane. The DO% was calculated using Eq. (4). The calculation considered the height of the (100) plane peak of the sample (H_A) and the heights H_P refer to the standard sample (CT02-0). In order to improve the determination of this parameter, the synthesis of each silica was repeated three times, and diffractograms were obtained at least twice for each sample.

$$DO(\%) = \frac{H_A}{H_P} \times 100 \quad (4)$$

Thermogravimetric analyses (TGA) of the silicas synthesized with CTMABr or CADMABr were performed in order to characterize the materials in terms of mass loss. These analyses employed a Shimadzu Model DTG-60H instrument, with heating from ambient temperature up to 800 °C at a rate of 10 °C min^{-1} in an oxidizing atmosphere (synthetic air, supplied at 40 mL min^{-1}).

Nitrogen physisorption was used to determine the specific areas of the as-synthesized catalysts. The procedure was also used for the silicas calcined at 500 °C for 5 h, in order to identify differences in the diameters and volumes of the pores, as well as the specific areas, of the silicas synthesized using the different surfactants (CTMABr and CADMABr). These analyses were performed using an ASAP 2020 instrument (Micromeritics). In the case of the non-calcined silicas, physisorbed water was first removed using a pretreatment at 40 °C under vacuum for 2 h, while the calcined silicas were pretreated at 200 °C under vacuum for 2 h. The specific area (S_{BET}) was determined by the Brunauer, Emmett, and Teller (BET) method, using the relative pressure (p/p_0) region between 0 and 0.3 for the calculation.

Scanning electron microscopy (SEM) analyses were performed using a Magellan 400 L microscope (FEI), operated at 25 kV. The samples were prepared by suspending a small quantity of material in acetone, sonicating for 1 h, and depositing drops of the suspension onto polished aluminum sample holders. Micrographs were collected varying the distance between the beam and the sample (from 2.2 to 3.7 mm) and the magnification (×20,000 and ×100,000).

The catalytic stability of the hybrid silicas was evaluated using the transesterification reaction of ethyl acetate with methanol [6,7]. The reaction was performed in a reactor with a capacity of 100 mL, at 50 °C, using 4% (m/m) of catalyst, a reaction time of 30 min, and an alcohol/ester molar ratio of 2. Each result was an average of at least three measurements.

3. Results and discussion

3.1. Synthesis of the CADMABr surfactant

The synthesis of cetylallyldimethylammonium bromide (CADMABr) provided high yields, generally around 92%. Given that this surfactant has been little studied, its composition was confirmed using CHN elemental analysis (Table 1).

Fig. 3 shows the expected chemical shifts (ppm) for the ^{13}C NMR analysis [18]. Fig. 4 presents the ^{13}C NMR spectrum obtained for the synthesized surfactant, which could be concluded to correspond to the formation of CADMABr.

Fig. 5 shows the small-angle X-ray scattering (SAXS) results obtained for the aqueous colloidal dispersions with different molar concentrations of the surfactants CTMABr and CADMABr (0.1, 0.2, and 0.4%). The peaks that can be seen in the spectra resulted from the formation of micelles and the effect of concentration.

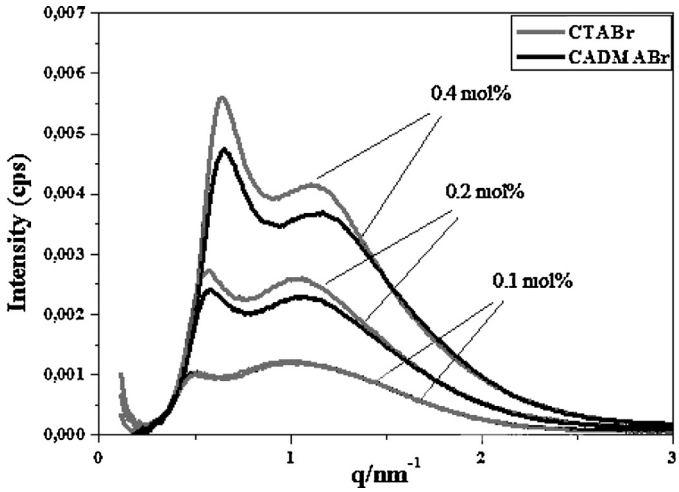

Fig. 5. SAXS spectra for different molar concentrations of CADMABr and CTMABr in water.

Table 2
Intermicellar distances calculated from the SAXS data. .

Concentration (mol%)		0.1	0.2	0.4
CADMABr	$q_{max}(nm^{-1})$	0.50	0.58	0.65
	$d_{intermicellar}$ (nm)	12.57	10.83	9.67
CTMABr	$q_{max}(nm^{-1})$	0.50	0.57	0.64
	$d_{intermicellar}$ (nm)	12.57	11.02	9.82

According to Aswal et al. [19], the first peak corresponds to X-ray scattering due to the presence of the micelles, while the second peak is due to scattering by the bromide ions surrounding the micelles. For the lowest molar surfactant concentration of the surfactants (0.1%), the spectra were virtually identical for both compounds. However, for molar concentrations of 0.2% and above, there were greater differences in intensity, and the two peaks became better defined.

It can be seen from Fig. 5 that for the same molar concentration, the scattering intensity obtained for CTMABr was generally greater than that for CADMABr. This suggests that a greater number of micelles were formed by CTMABr than CADMABr. On the other hand, for the same concentration, the average distance between the micelles formed in the two systems were very similar (Table 2). Furthermore, both followed the same trend: there was a shift towards larger scattering vectors (q) as the surfactant concentration was increased, indicating a reduction of intermicellar distances (Eq. (2)).

3.2. Irradiated aqueous dispersions of CADMABr

The effects of the γ radiation on the aqueous dispersions of CADMABr were characterized using ^{13}C NMR. Fig. 6 shows the spectra of the dispersion after irradiation at 48kGy dose by γ radiation.

Comparison of the ^{13}C signals of the alkyl groups of non-irradiated CADMABr (Fig. 4) with those of the irradiated dispersion (Fig. 6) showed that the signals of the former were also present in the latter, with similar chemical shifts (ppm), indicating that the gamma radiation did not cause degradation of the molecule. However, the irradiated sample showed a peak at a chemical shift of 45 ppm, which was not present in the case of the non-irradiated sample. Furthermore, the intensity of this signal increased with increasing radiation dose (88, 128, and 160 kGy). According to Silverstein et al. [18], this indicates that there was the formation of

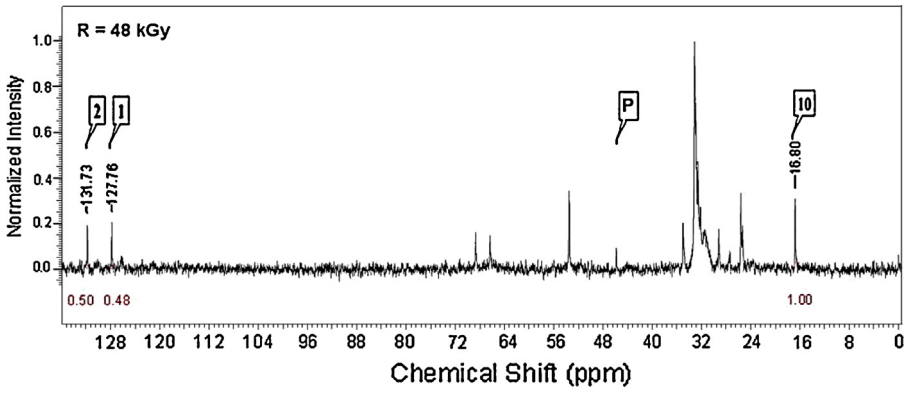

Fig. 6. ^{13}C NMR spectra of the dispersions containing CADMABr irradiated with a dose of 48 kGy (R_{48}-CADMA).

Table 3
Olefinic carbon A1 areas, according to radiation absorbed dose.

Dose (kGy)	C=C (A1)
0	2.00
16	1.67
48	0.98
88	0.61
128	0.16
160	0.16

a tertiary carbon group, resulting from polymerization of the allyl group of the surfactant. At the same time, the peaks with chemical shifts of 131 and 127 ppm, corresponding to C2 and C1 of the double bond of the allyl group (Fig. 3), showed decreases in intensity as the radiation dose was increased, indicating a greater degree of polymerization of CADMABr. Another indication of the polymerization of the surfactant was an increase in viscosity with increasing dose, with formation of a gelatinous substance at the highest dose used in this study (160 kGy). In terms of visual appearance, the originally colorless dispersion became slightly turbid at a radiation dose of 88 kGy and opaque at the maximum dose used. Table 3 shows the A1 values corresponding to the sums of the areas of the olefinic carbons (carbons 1 and 2 in Fig. 3), as a function of the radiation dose, where it can be seen that the values decreased due to the polymerization.

For each sample, the values of areas A1 and A2 were substituted into Eq. (1) to obtain the degree of polymerization of CADMABr surfactant according to γ radiation dose (Fig. 7).

As showed in Fig. 7, for the irradiation with a dose of 128 kGy (R_{128}-CADMA) to an aqueous dispersion containing 0.2 mol% CADMABr resulted in a degree of polymerization of 92%, and that there was no further significant change after increasing the dose to 160 kGy. This stabilization in the degree of polymerization could have been due to the decrease in concentration of the monomer and the high viscosity of the medium.

A similar system was studied by Rodríguez et al. [20], using an aqueous dispersion containing 65% by weight of ADDABr, a surfactant with the same head as CADMABr, but with a shorter carbon chain composed of 12 atoms. However, a degree of polymerization of only 35% was obtained after exposure to a 55 kGy dose of γ radiation, which was much lower than achieved in the present work.

3.3. Synthesis and properties of CADMA-MCM-41

Comparison of the diffractogram obtained for the sample synthesized in 2 h, using CADMABr with Beck et al. [8] (CD02-0 in Fig. 8), showed that it followed the same pattern, with four well-defined peaks corresponding to the (100), (110), (200), and (210)

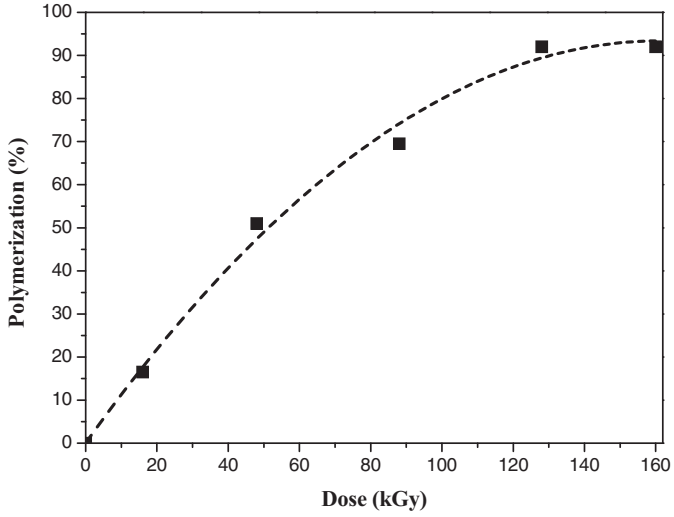

Fig. 7. Degree of polymerization obtained in liquid medium.

planes typical of the MCM-41 structure. This indicates that under these conditions, substitution of the CTMA cation by CADMA did not have any major influence on the structural properties of the hybrid silica.

Fig. 8 shows diffractograms for the silicas obtained at 30 °C, with synthesis times of between 2 and 48 h, using CADMABr as the surfactant.

All the conditions tested resulted in the formation of MCM-41. As can be seen from Fig. 8, and quantified as DO% (Eq. (4)) in Table 5, a longer synthesis time resulted in increased intensity of the peak for the (100) diffraction plane, with maximum intensity achieved using a period of 24 h. From Table 5, it can also be seen that as the synthesis time increased, the interplanar distance (Eq. (3)) tended to decrease. Possible explanations are a smaller pore diameter or reduced thickness of the silica wall.

In terms of intensity, the diffractograms obtained for the silicas showed behavior different to that observed for the liquid phase (Fig. 5), where the peaks for the colloidal dispersions of CADMABr were less intense, compared to those for CTMABr. These differences, in terms of both DO% and the intensity of the peaks, could have been due to greater difficulty in organization of the CADMA cations within the pores of the silica, due to the asymmetry of its head resulting from the presence of the allyl group.

The catalytic activities of the CTMA-MCM-41 and CADMA-MCM-41 silica hybrids were evaluated using the monoester transesterification reaction model, considering the effects of surfactant type and synthesis time.

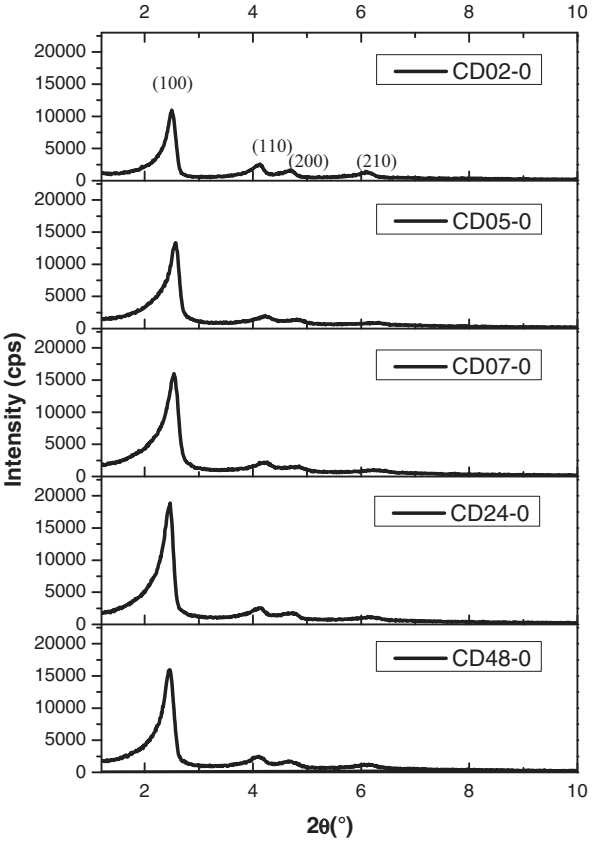

Fig. 8. X-ray diffractograms for the CADMA-MCM-41 silica prepared at 30 °C using different synthesis times.

Table 4
Evaluation of the hybrid silicas used in the catalytic transesterification.

Catalyst	Conversion (%)	
	1st use	4th use
CT02-Y	43.3	23.0
CD02-Y	48.0	21.7
CD05-Y	46.1	19.1
CD07-Y	45.8	20.4
CD24-Y	44.6	17.6
CD48-Y	44.1	18.9

Conditions: T = 50 °C; t = 30 min; wt% = 4%. The average standard deviation of the catalytic activities was 3%.

Table 5
Structural parameters of the silicas (for the (100) plane), calculated from the X-ray diffraction results.

	As-synthesized (Y = 0)			After 4th use (Y = 4)	
Silica	DO%	2θ (°)	d_{100} (nm)	DO%	2θ (°)
CT02-Y	100	2.50	3.53	33.6	3.02
CD02-Y	91.5	2.50	3.53	33.3	3.16
CD05-Y	111.5	2.57	3.44	30.8	2.74
CD07-Y	133.6	2.54	3.48	21.8	2.97
CD24-Y	157.7	2.47	3.58	13.1	3.27
CD48-Y	133.5	2.46	3.59	10.4	3.31

Table 4 gives the conversions of ethyl acetate to methyl acetate achieved in successive reuses of MCM-41 synthesized during 2 h at 30 °C with CADMABr and CTMABr (CD02-Y and CT02-Y, respectively), and the conversions for the materials prepared with CADMABr using different synthesis times (CDXX-Y, where: XX = 02, 05, 07, 24, and 48 h; Y = 0 to 4 reuses of the catalyst).

The initial activity (43% conversion) of the CT02-0 silica synthesized with the standard surfactant (CTMABr) (Table 4) was very similar to values reported previously [7]. During reuse, there was an appreciable reduction in catalytic activity, as also observed in the earlier work, which could be explained by leaching of the surfactant [4,5] and consequent loss of the basic sites. Table 4 also shows the activity of the CD02 silica synthesized using the new surfactant (CADMABr) containing the basic sites shown in Fig. 9. Compared to the standard silica (synthesized using CTMABr), the activity of CD02 was slightly higher during the first use. However, as for CT02, the conversion achieved with CD02 diminished with successive reuse, probably due to the leaching of cations mentioned previously. Table 4 shows the activities of the silicas obtained using the CADMA cations and different synthesis times, from which it can be seen that the activity decreased as the synthesis time was increased. Curiously, a longer synthesis time improved the degree of organization of these silicas (Table 5), but not their catalytic activity or stability.

Fig. 10 shows the X-ray diffractograms obtained for the CT02-Y and CD02-Y silicas, immediately after preparation and after the fourth use, whose catalytic activities are shown in Table 4.

The X-ray diffractograms of both silicas revealed appreciable losses of organization, with disappearance of the peaks corresponding to planes (110), (200), and (210), and reduction and broadening of the main peak corresponding to the (100) plane. This loss of organization was associated with the leaching of CTMA or CADMA cations from the pores, leading to lower pore density in the hexagonal structure and fewer catalytic sites ($\equiv SiO^-$) available for the reaction.

The structural characteristics of the catalysts, as-synthesized and after the fourth use, are provided in Table 5, together with the corresponding DO% values. The data showed that the degree of organization decreased from the first to the fourth use. The standard sample showed a decrease of 37% after the fourth use, while the loss of organization of the CADMA samples reached 78% for the sample prepared using an agitation time of 24 h. All the samples synthesized at 30 °C, independent of the surfactant used, showed shifts to greater angles after successive uses, indicating possible contraction of the pores, and the degree of organization decreased to below 42% for all the materials. As diffractograms of the silicas after the fourth catalytic use did not present all characteristic peaks of MCM-41 structure, the interplanar distance (d_{100}) can not be calculated (Table 5).

Evaluation of changes in the morphology of the silica produced with the modified surfactant, following the catalytic activity evaluations, was conducted by SEM analysis of the hybrid silica prior to use (sample CD02-0) and after the fourth use (sample CD02-4) (Fig. 11).

Fig. 11 shows the formation of tubes that intermingle in an irregular and non-uniform fashion (snakelike). Similar morphology was found after successive reuses of the material in the transesterification reaction. The morphology of CADMA-MCM-41 was very different to that of CTMA-MCM-41 described previously, which was poorly defined and showed the presence of small spherical particles [6].

Fig. 12 shows the thermograms obtained under an oxidizing atmosphere for samples prepared using CADMABr and CTMABr, as-synthesized or after four uses as catalysts in the transesterification reaction.

The thermogram profiles obtained for the silicas synthesized with CADMABr were similar to those reported by Zhao et al. [21] for materials synthesized with CTMABr. There were four regions of mass loss, which according to Zhao et al. [21], under an oxidizing atmosphere correspond to the desorption of physically adsorbed water (R1), Hoffman decomposition of the surfactant (R2), combustion of residual carbon (R3), and dehydroxylation of silanols

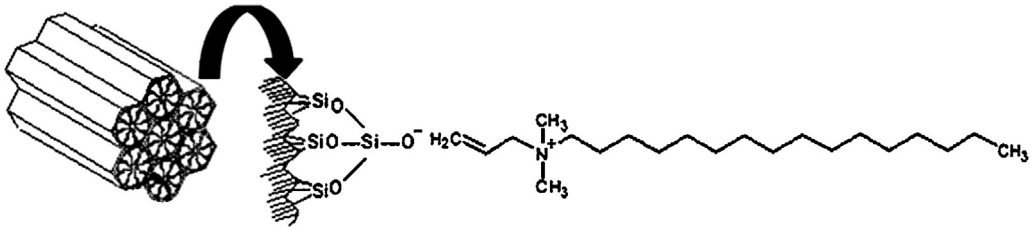

Fig. 9. Representation of the siloxy site of CADMA-MCM-41.

Table 6
Mass losses of the silicas containing CTMA and CADMA, synthesized at 30 °C, in each temperature region, before and after use as catalysts.

Temperature (°C)	T < 140	140 < T < 320	320 < T < 450	T > 450	R2 + R3 (%)	SiO_2 (%)	$\frac{M_{cation}}{M_{silica}}$
Silica	R1 (%)	R2 (%)	R3 (%)	R4 (%)			
CT02-0	4.5	46.5	6.4	4.2	52.9	38.4	0.29
CT02-4	4.7	23.7	7.6	5.0	31.3	59.0	0.11
CD02-0	4.2	37.4	13.2	7.5	50.6	37.7	0.26
CD02-4	4.4	16.7	10.8	8.4	27.5	59.7	0.09

(R4). However, thermal analyses of CADMA-MCM-41 samples performed under oxidizing and inert atmospheres generated identical thermograms. Hence, in the case of this type of sample, there were no oxidation reactions and the mass loss in the R3 region was probably due to desorption of components associated with decomposition of the surfactant. The values of the mass losses in each region are given in Table 6.

Table 6 also lists the mass losses of organic material (sum of regions R2 and R3) and the percentage of silica contained in each sample (% SiO_2). This last value was obtained by subtracting the sum of the mass losses in the four regions from the initial mass (100%). The values in the final column were obtained by division of the molar masses shown in the two preceding columns ((R2 + R3)/SiO_2). These values show that the hybrid silica synthesized with $CADMA^+$ (CD02-0) was characterized by a cation/SiO_2 molar ratio smaller than that for the sample prepared with $CTMA^+$. The results therefore suggested that the pores formed by $CADMA^+$ possessed a smaller number of cations, compared to the pores formed by $CTMA^+$. The data (Table 6, column R2 + R3) showed that after the fourth use as catalysts in the transesterification reaction, these hybrid silicas lost around 20% of the organic cations present in the original material. The reduction in the content of organic material was accompanied by a strong loss of catalytic activity (Table 4). The loss was therefore associated with a diminution in the number of siloxy anions (Fig. 9), which were the catalytic sites, because they were transformed into silanols that were inactive in the reaction.

Table 6 shows that for both the original and reused materials, the loss of mass in region R2 was smaller for the silica containing $CADMA^+$, compared to that containing $CTMA^+$. The inverse occurred for region R3, where for both the as-synthesized and used materials, the loss was greater for the silica containing $CADMA^+$. A likely explanation for this behavior lies in differences between the products formed during decomposition of the cations. According to Zhao et al. [21], Hoffman decomposition of the CTMA cation occurs according to Reaction (1):

$$C_{16}H_{33}(CH_3)_3N^+ \rightarrow C_{14}H_{29}CH{=}CH_2 + (N(CH_3)_3) + H^+ \quad (1)$$

It is therefore expected that decomposition of the CADMA cation should proceed according to Reaction (2):

$$C_{16}H_{33}(CH_3)_2N^+(CH_2CH{=}CH_2) \rightarrow C_{14}H_{29}CH{=}CH_2 + CH_3 C{\equiv}CH + (HN(CH_3)_2) + H^+ \quad (2)$$

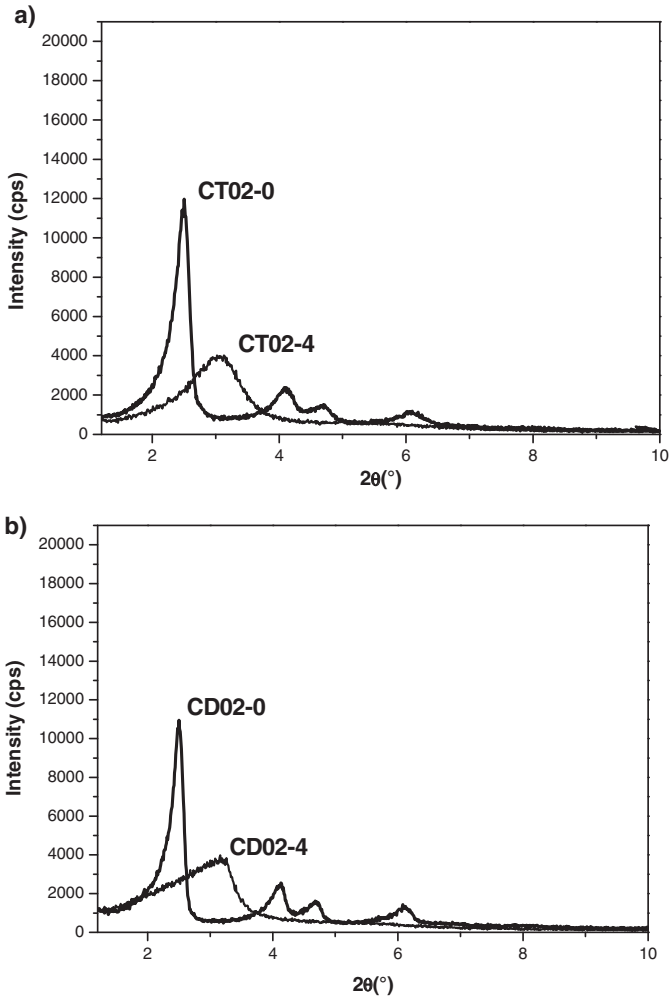

Fig. 10. X-ray diffractograms of the silicas, as-synthesized and after the fourth use: (a) CT02-Y; (b) CD02-Y.

The main difference between the products of decomposition of the CADMA cation, relative to CTMA, is the formation of an alkyne (propyne) derived from the allyl radical. At the temperature at which decomposition of CADMA occurs (region R2), the alkyne polymerizes, forming a compound that is more stable than the cation in question. The formation of this more stable polymer

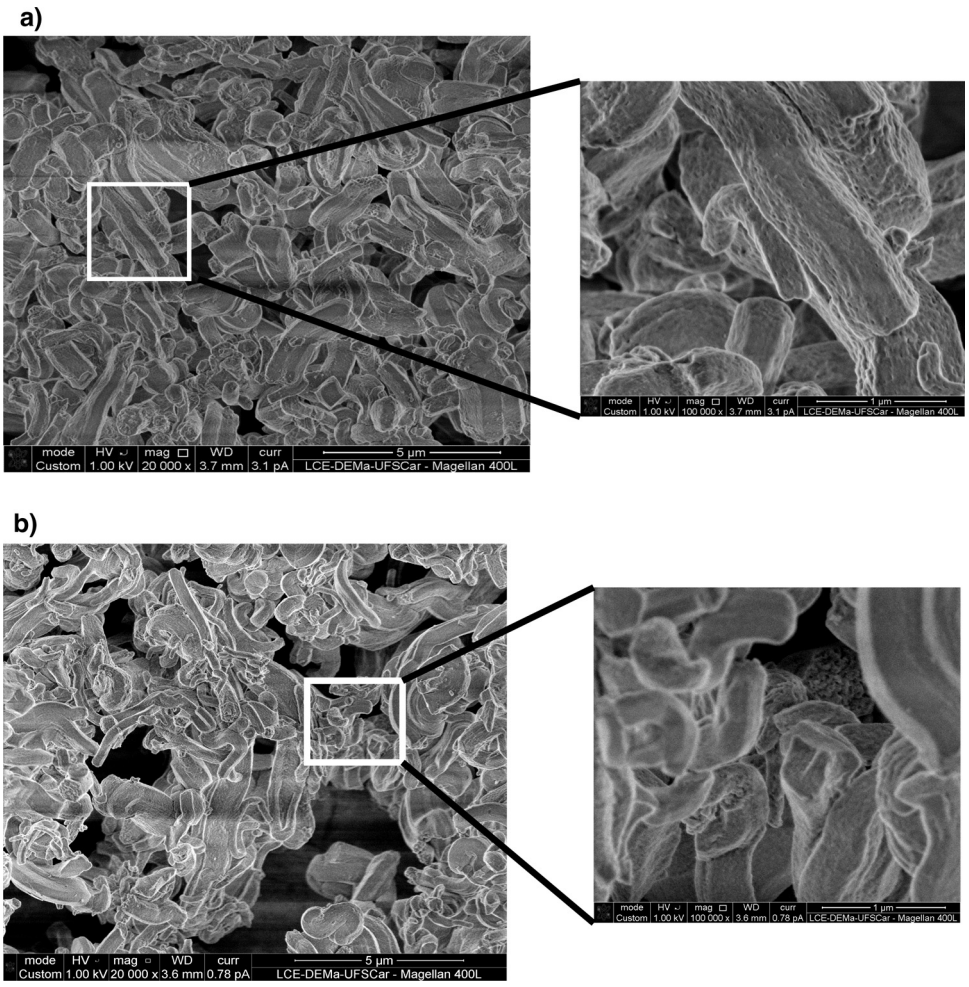

Fig. 11. Scanning electron micrographs of CADMA-MCM-41: (a) as-synthesized (CD02-0); (b) after the fourth use (CD02-4).

explains the lower mass loss in region R2. Its subsequent oxidation, at higher temperatures, leads to increased mass loss in region R3, relative to the mass loss in the same region obtained for the silica containing the CTMA cation.

Finally, in region R4, corresponding to the formation of water by condensation of silanols, greater mass loss was observed for the original silica produced using the CADMA cation (CD02-0), compared to the use of CTMA, suggesting that the former contained more silanols. Similar differences were also observed between the samples used catalytically four times. These findings can be explained by the smaller quantity of cations in the sample synthesized with CADMA, which consequently contained more hydroxyls.

Fig. 13 shows the N_2 physisorption isotherms obtained for the hybrid silicas synthesized with CTMABr (CT02-Y) and CADMA (CD02-Y), as-synthesized (Y = 0) and after four or five uses (Y = 4 or 5) as catalyst in the transesterification reaction.

The isotherms of both materials (Fig. 13) showed the same behavior, similar to type II, according to the BET classification. An explanation for this behavior, which is typical of nonporous materials, is the occlusion of the mesopores of these silicas by CADMA or CTMA cations. The BET specific areas of the two silicas that had not been used in the catalytic tests (CT02-0 and CD02-0) were approximately the same: $4.2 \pm 0.1\ m^2/g$. The silicas that had been used in the catalysis showed a slight increase in the average specific area, to $6.7 \pm 0.9\ m^2/g$. As shown in Table 6 (columns R2 + R3), during use these silicas lost around 20% of the original organic material. At the same time, there was a decrease in catalytic activity after use (Table 4). However, the adsorption isotherms showed that this loss did not result in emptying of the mesopores, even after five uses in the model reaction. These results suggest that the organic material that was leached from the hybrid silicas was not extracted from the mesopores, but was released from the external surface. Hence, the siloxy sites that were deactivated during the catalytic tests were present on the external surfaces of the catalysts. This conclusion differs from the suggestion of Kubota et al. [10] that the catalytic reaction occurred in the mouths of the mesopores.

Table 7
N2 physisorption results for the calcined silicas.

	MCM-41 (CTMA)	MCM-41 (CADMA)
D_p (nm)	2.0	2.5
V_p (cm^3/g)	0.85	1.02
S_{BET} (m^2/g)	1533	1492

Table 7 shows the N_2 physisorption results for the calcined silicas produced using the CTMA and CADMA cations. The results suggest that the diameters (D_p) of the pores formed by the CADMA cation were larger than those formed by the CTMA cation, in agreement with the SAXS data for the aqueous dispersions and as shown schematically in Fig. 14. This was probably because the micelles formed by the CADMA cation possessed greater diameters, due to the substitution of a methyl group by an allyl group (Fig. 1). This hypothesis is supported by the results obtained for the physisorption of N_2 onto the calcined silicas (Table 7). Fig. 14 provides a

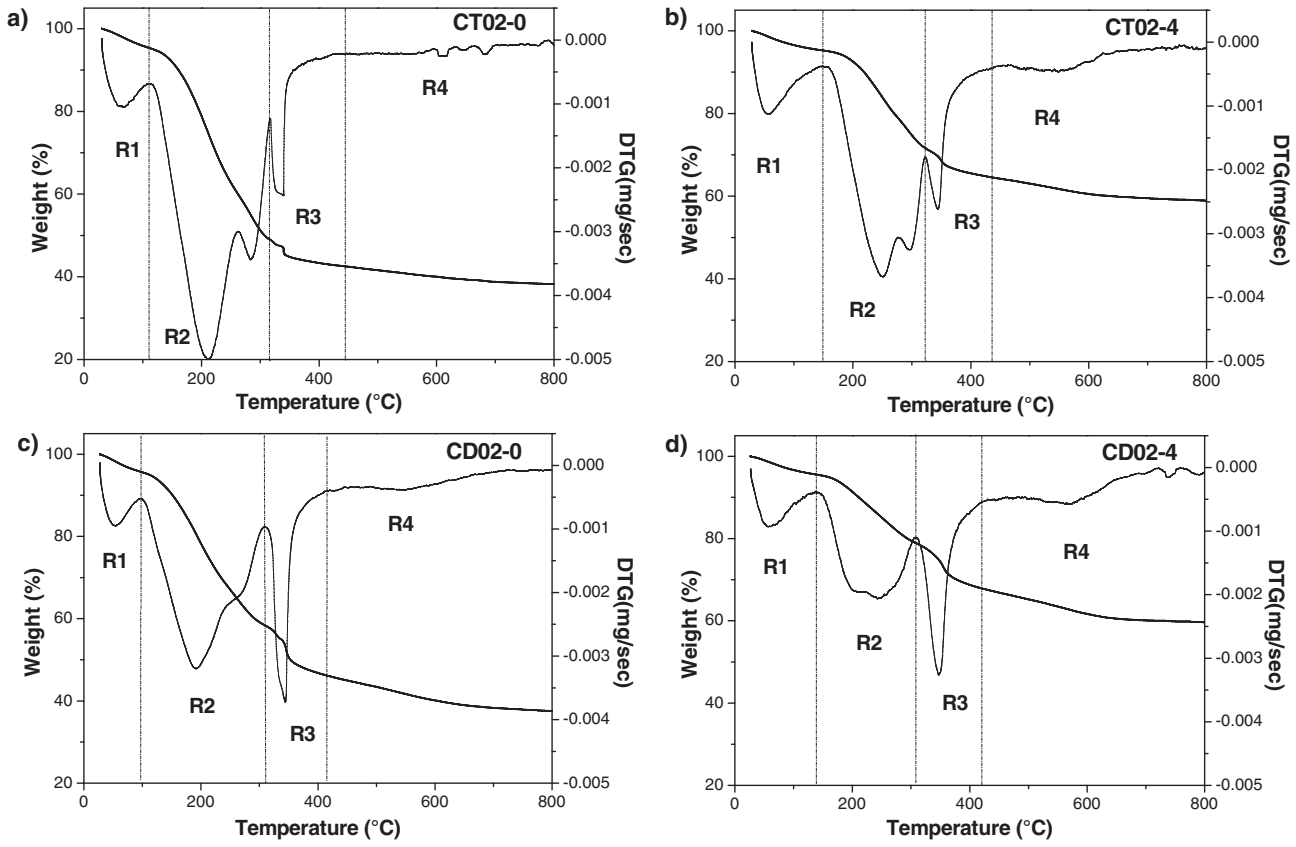

Fig. 12. Thermogravimetric analyses in an oxidizing atmosphere of (a and c) the as-synthesized silicas prepared with CTMABr and CADMABr, and (b and d) after four uses in the transesterification reaction.

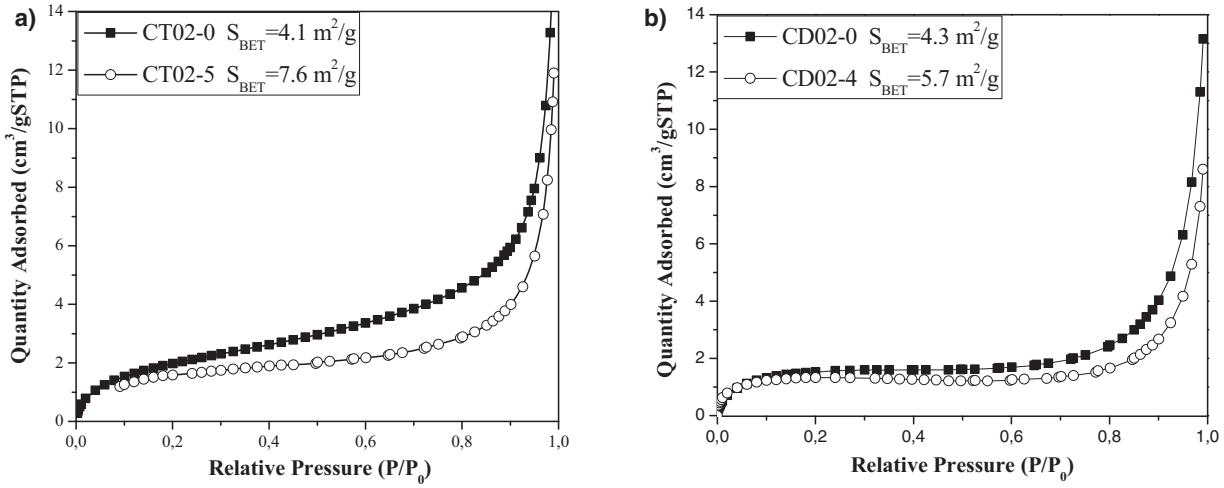

Fig. 13. Physisorption of N_2 by (a) CTMA-MCM-41 and (b) CADMA-MCM-41, as-synthesized or after the fifth or fourth use as catalyst.

schematic representation of these SAXS results, with micelles the same distance apart but with different diameters.

Comparison of the X-ray diffractograms for the CADMA-MCM-41 silica subjected to the lower radiation dose (CD02-R_{48}-0) with those for the silica synthesized in the same batch, but not subjected to radiation (CD02-0) (Figs. 15 and 10b), it can be seen that all the peaks were shifted to a smaller 2θ angle. This indicated that submission of this hybrid silica containing CADMA surfactant in its pores to irradiation resulted in greater interplanar distances. This expansion was probably caused by polymerization of the surfactant.

The diffractograms (Fig. 15) also showed that increasing the radiation dose to 128 kGy did not cause any change in the 2θ angles of the peaks. However, there were increases in the intensities of all the peaks corresponding to the characteristic planes of MCM-41, suggesting that increased radiation intensity led to the formation of a mesoporous MCM-41 silica that was more organized. Table 9 gives the degrees of organization (DO%) of the silicas, calculated using Eq. (4), indicating that radiation resulted in a degree of organization that was more than twice the value obtained for the standard sample.

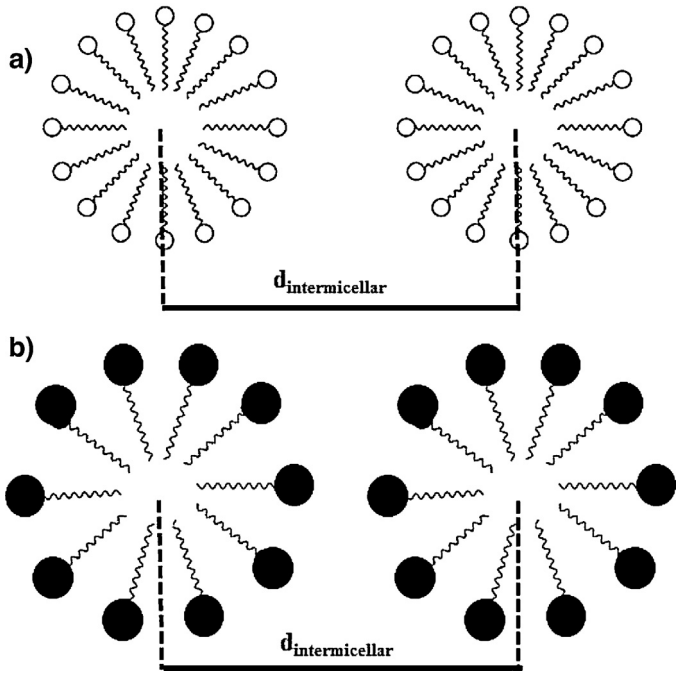

Fig. 14. Representation of the intermicellar distance for (a) CTMABr and (b) CADMABr.

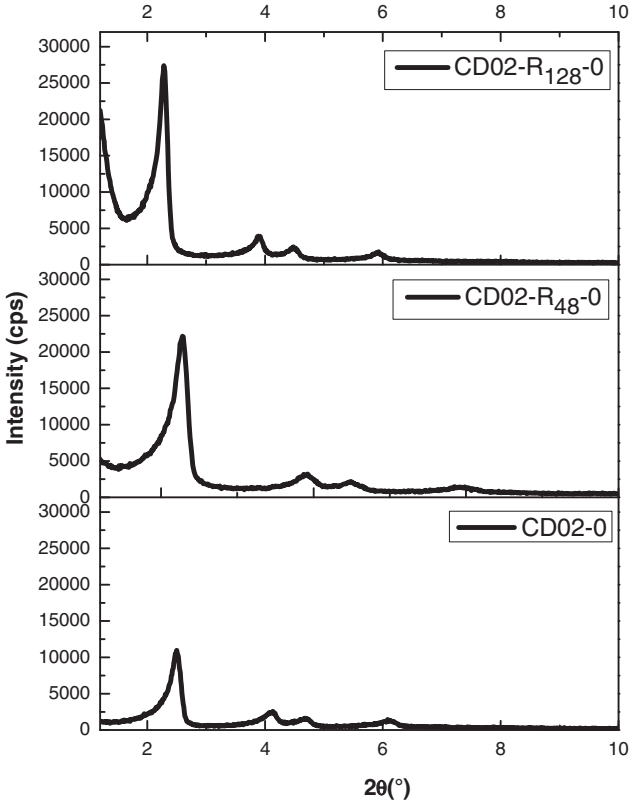

Fig. 15. X-ray diffractograms of CADMA-MCM-41 silica, without irradiation or treated with γ radiation doses of 48 and 128 kGy.

Scanning electron microscopy revealed no perceptible differences between the irradiated and non-irradiated silicas in terms of particle shape (Fig. 11).

After irradiation, evaluation was made of the catalytic properties of the hybrid silicas containing CADMA cations (Table 8).

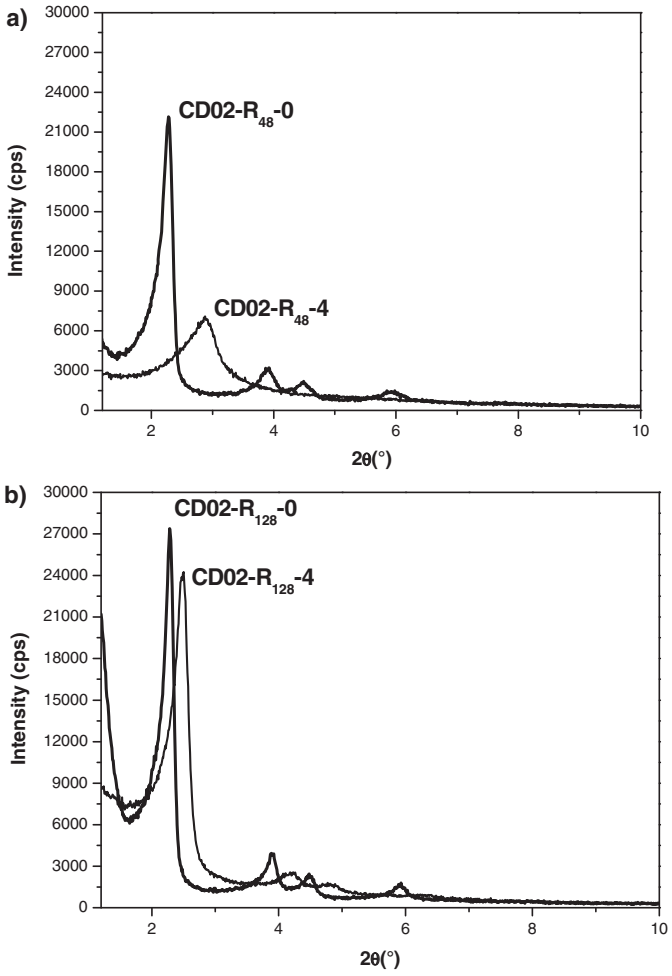

Fig. 16. X-ray diffractograms of the CD02-0 silicas, before use and after the 4th use as catalyst, submitted to γ radiation doses of (a) 48 kGy and (b) 128 kGy.

Table 8
Catalytic evaluation of the irradiated hybrid silicas.

Catalyst	Conversion (%)[a]	
	1st use	4th use
CD02- R_{48}	44.9	21.6
CD02- R_{128}	30.4	4.3

[a] Standard deviations of ±1.5%.

Comparison of the catalytic activities of the irradiated hybrid silicas with the non-irradiated silica (CD02-0 in Table 4) showed that the radiation caused a decrease in the initial activity. Furthermore, the activity decreased substantially with increasing radiation dose. The substantial loss of activity in the irradiated catalysts indicated that polymerization resulted in most of the active sites not being accessible for the reaction.

The catalysts were characterized by X-ray diffraction before the first use and after the fourth use in the transesterification reaction. The diffractograms obtained are shown in Fig. 16. Fig. 16a shows that although the silica obtained with the lowest radiation dose (CD02-R_{48}-0) presented a better degree of organization than the original silica (Fig. 10b, sample CD02-0), it suffered a substantial loss of organization after the 4th use as a catalyst (CD02-R_{48}-4). Fig. 16b shows that when the radiation dose was increased to 128 kGy, the degree of organization of this sample (CD02-R_{128}-4) also decreased after the 4th use as a catalyst, but the degree of organization was greater than that of the original sample. In contrast

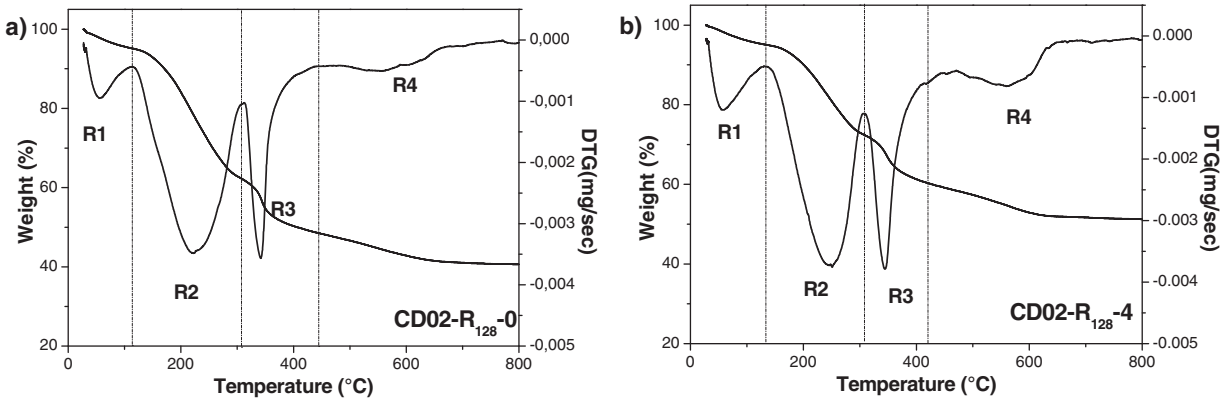

Fig. 17. Thermogravimetric analysis in an oxidizing atmosphere of the silica irradiated with 128 kGy: (a) as-synthesized and (b) after the 4th use.

Table 9
Structural parameters for the (100) plane of the silicas, calculated from the X-ray diffraction data.

Silica	As-synthesized (Y = 0)			After 4th use (Y = 4)		
	DO%	2θ (°)	d_{100} (nm)	DO%	2θ (°)	d_{100} (nm)
CD02-R_{48}-Y	185.2	2.28	3.87	59.3	2.88	–
CD02-R_{128}-Y	228.8	2.28	3.87	202.7	2.50	3.53

Table 10
Mass losses of the irradiated silicas in each temperature region, before and after use as catalysts.

Temperature (°C)	T < 140	140 < T < 320	320 < T < 450	T > 450	R2 + R3 (%)	SiO_2 (%)	$\frac{M_{cation}}{M_{silica}}$
Silica	R1 (%)	R2 (%)	R3 (%)	R4 (%)			
CD02-R_{48}-0	5.3	36.9	13.0	7.2	49.9	37.6	0.26
CD02- R_{48}-4	4.9	16.0	11.5	8.1	27.5	59.5	0.09
CD02-R_{128}-0	6.2	31.8	13.6	7.9	45.4	40.5	0.22
CD02-R_{128}-4	5.1	22.7	13.0	8.2	35.7	51.0	0.14

to all the other samples evaluated, the X-ray diffractogram of this sample (CD02-R_{128}-4) retained the three peaks corresponding to the (100), (110), and (200) diffraction planes characteristic of MCM-41, with a small shift towards larger angles indicating contraction of the material.

Table 9 summarizes the structural parameters of the irradiated hybrid silicas whose X-ray diffractograms are shown in Fig. 16.

The original silica showed a sharp loss in the degree of organization (58.2%) after the 4th use as a catalyst (CD02-4) (Table 5). However, increasing the radiation dose to 128 kGy not only increased the degree of organization of the unused sample, but also led to a smaller loss in the degree of organization (26%) after the 4th use as a catalyst (CD02-R_{128}-4) (Table 9). In this case, the interplanar distance (d_{100}) was calculated, because the CD02-R_{128}-4 silica presented all characteristic peaks of MCM-41 structure.

Thermal analyses were used to determine the influence of γ radiation on the retention of organic material contained in the hybrid silicas used as catalysts. Fig. 17 shows the thermograms (obtained under an oxidizing atmosphere) of the silica subjected to a dose of 128 kGy, before use (CD02-R_{128}-0) and after the 4th use as a catalyst (CD02-R_{128}-4). The thermogram profiles of the irradiated silica were similar to those of the non-irradiated silica (Fig. 12), with four mass loss regions. The mass losses in each region are given in Table 10, together with the percentage losses of organic material (R2 + R3), silica (SiO_2%), and the cation/SiO_2 molar ratios for each sample. Table 10 also shows the results for the hybrid silica subjected to a smaller dose of γ radiation (48 kGy), for which the thermograms were similar to those of Fig. 17.

The hybrid silica irradiated with 48 kGy showed cation/SiO_2 molar ratios of 0.26 and 0.09 for CD02-R_{48}-0 and CD02-R_{48}-4, respectively, which were identical to the values for the non-irradiated hybrid silica (CD02-0 and CD02-4, Table 6). Therefore, this radiation dose did not cause any modifications to the organic compounds present within the channels of the CADMA-MCM-41 silica.

When the γ radiation dose was increased to 128 kGy, the unused silica catalyst (CD02-R_{128}-0) showed a smaller cation/SiO_2 molar ratio, compared to the non-irradiated silica (CD02-0), with values of 0.22 and 0.26, respectively. This could indicate that a high radiation dose caused degradation and partial loss of organic material present on the surface or within the channels of the MCM-41. However, after being used four times as a catalyst (CD02-R_{128}-4), this silica presented a cation/SiO_2 molar ratio of 0.14, which was higher than the value of 0.09 found for CD02-4 (Table 6). After use as a catalyst, the irradiated sample therefore retained about 80% of the organic cations originally present in the silica, while the non-irradiated sample retained only 54%. These findings suggest that this dose of γ radiation induced polymerization of the CADMA cations within the silica, resulting in reduced leaching after the fourth use in the catalytic reaction.

4. Conclusions

Optimization of the synthesis of CADMABr surfactant, using an adaptation of the method described by Paleos et al. [13], achieved a 92% yield of solid after only one hour at 65 °C. SAXS analysis of aqueous dispersions of CADMABr confirmed the formation of micelles and behavior in water similar to that of CTMABr, indicating the suitability of the new surfactant for formation of MCM-41.

The CADMABr surfactant was used for silica synthesis, and XRD analysis confirmed formation of the MCM-41 structure. Combination of N_2 physisorption and SAXS results indicated that the micelles and the pores formed using the CADMA cation possessed diameters that were larger than those obtained using the CTMA cation. The CADMA-MCM-41 hybrid silica was active in the catalytic transesterification, but nonetheless showed leaching of the cations during use.

Increasing the γ radiation dose from 128 to 160 kGy resulted in no increase in the degree of polymerization of aqueous dispersions containing the CADMABr surfactant, which remained at 92%, possibly due to dilution of monomeric cations in the polymer matrix.

There was a pronounced loss of organization of the CADMA-MCM-41 silica when it was used as a catalyst in the transesterification reaction. However, treatment of this silica with a 128 kGy radiation dose increased the degree of organization of the MCM-41, which was maintained after use as a catalyst.

In addition to improved structural stability, exposure to γ radiation increased the retention of cations in the silica after its use as a catalyst, probably due to their polymerization within the CADMA-MCM-41 silica. However, greater cation retention did not lead to stabilization of the catalyst, suggesting that polymerization might have hindered access to the catalytic sites.

Acknowledgements

The authors thank CNPq and CAPES for financial support, the Brazilian National Synchrotron Light Laboratory (LNLS) for the small-angle X-ray scattering (SAXS) analyses, and the Nuclear and Energy Research Institute (IPEN/USP, São Paulo) for the sample irradiations for polymerization at the Multipurpose Gamma Irradiation Facility.

References

[1] F. Ma, M.A. Hanna, Bioresour. Technol. 70 (1999) 1–15.
[2] E. Lotero, Y. Liu, D.E. Lopez, K. Suwannakarn, D.A. Bruce, J.G.S. Goodwin Jr., Ind. Eng. Chem. Res. 44 (2005) 5353–5363.
[3] K.G. Georgianni, A.P. Katsoulidis, P.J. Pomonis, M.G. Kontominas, Fuel Process. Technol. 90 (2009) 671–676.
[4] L. Martins, T.J. Bonagamba, E.R. de Azevedo, P. Bargiela, D. Cardoso, Appl. Catal. A 312 (2006) 77–85.
[5] D.P. Fabiano, B. Hamad, D. Cardoso, N. Essayem, J. Catal. 276 (2010) 190–197.
[6] J.A. Araújo, F.T. Cruz, I.H. Cruz, D. Cardoso, Microporous Mesoporous Mater. 180 (2013) 14–21.
[7] F.T. Cruz, D. Cardoso, Quim. Nova 37 (2014) 761–765.
[8] J.S. Beck, J.C. Vartuli, W.J. Roth, M.E. Leonowicz, C.T. Kresge, K.D. Schmitt, C.T.-W. Chu, D.H. Olson, E.W. Sheppardt, S.B. Mccullen, J.B. Higgins, J.L. Schlenkert, J. Am. Chem. Soc. 14 (1992) 10834–10843.
[9] J.C. Vartuli, K.D. Schmitt, C.T. Kresge, W.J. Roth, M.E. Leonowicz, S.B. Mccullen, S.D. Hellring, J.S. Beck, J.L. Schelenker, D.H. Olson, E.W. Sheppard, Chem. Mater. 6 (1994) 2317–2326.
[10] Y. Kubota, Y. Nishizaki, H. Ikeya, M. Saeki, T. Hida, S. Kawazu, M. Yoshida, H. Fujii, Y. Sugi, Microporous Mesoporous Mater. 70 (2004) 135–149.
[11] S.M. Hamid, D.C. Sherrington, Polymer 28 (1987) 325–331.
[12] D. Cardoso, L.L. Silva, I.H. Cruz, J. Araújo Brazil, (2014), Patent BR, 10, 2014, 0024301.
[13] C.M. Paleos, P. Dais, N.R.C. Angelos Malliaris, J. Polym. Sci. 22 (1984) 3383–3391.
[14] C. Tribet, R. Gaboriaud, P. Gareil, J. Chromatogr. 608 (1992) 131–141.
[15] K.M. McGrath, C.J. Drummond, Colloid Polym. Sci. 274 (1996) 316–333.
[16] K. Schumacher, M. Grün, K.K. Unger, Microporous Mesoporous Mater. 27 (1999) 201–206.
[17] V.K. Aswal, P.S. Goyal, Chem. Phys. Lett. 357 (2002) 491–497.
[18] R.M. Silverstein, F.X. Webster, D. Kiemle, Spectrometric Identification of Organic Compounds, 7th edition, John Wiley & Sons, Hoboken, 2005, pp. 198–221.
[19] V.K. Aswal, P.S. Goyal, H. Amenitsch, S. Bernstorff, J. Phys. 63 (2004) 333–338.
[20] J.L. Rodríguez, J.F.A. Soltero, J.E. Puig, P.C. Schulz, M.L. Espinoza-Martínez, O. Pieroni, Colloid Polym. Sci. 277 (1999) 1215–1219.
[21] X.S. Zhao, G.Q. Lu, A.K. Whittaker, G.J. Millar, H.Y. Zhu, J. Phys. Chem. B 101 (1997) 6525–6531.